J. metamorphic Geol., 2005, **23,** 19–28 doi:10.1111/j.1525-1314.2005.00555.x

Experimental deformation of partially melted granite revisited: implications for the continental crust

C. L. ROSENBERG AND M. R. HANDY
Department of Geological Sciences, Freie Universität Berlin, Malteserstr. 74-100, 12249 Berlin, Germany (cla@zedat.fu-berlin.de)

ABSTRACT A review and reinterpretation of previous experimental data on the deformation of partially melted crustal rocks reveals that the relationship of aggregate strength to melt fraction is non-linear, even if plotted on a linear ordinate and abscissa. At melt fractions, $\Phi < 0.07$, the dependence of aggregate strength on Φ is significantly greater than at $\Phi > 0.07$. This melt fraction ($\Phi = 0.07$) marks the transition from a significant increase in the proportion of melt-bearing grain boundaries up to this point to a minor increase thereafter. Therefore, we suggest that it is the increase of melt-interconnectivity that causes the dramatic strength drop between the solidus and a melt fraction of 0.07. We term this drop the 'melt connectivity transition' (MCT). A second, less-pronounced strength drop occurs at higher melt fractions and corresponds to the breakdown of the solid (crystal) framework. This is the 'solid-to-liquid transition' (SLT), corresponding to the well known 'rheologically critical melt percentage'. Although the strength drop at the SLT is about four orders of magnitude, the absolute value of this drop is small compared with the absolute strength of the unmelted aggregate, rendering the SLT invisible in a linear aggregate strength *v.* melt-fraction diagram. On the other hand, the more important MCT has been overlooked in previous work because experimental data usually are plotted in logarithmic strength *v.* melt-fraction diagrams, obscuring large strength drops at high absolute strength values. We propose that crustal-scale localization of deformation effectively coincides with the onset of melting, pre-empting attainment of the SLT in most geological settings. The SLT may be restricted to controlling flow localization within magmatic bodies, especially where melt accumulates.

Key words: crustal weakening; experimental deformation; melt; partially melted granite; rheologically critical melt percentage.

INTRODUCTION AND BRIEF REVIEW OF THE RHEOLOGICALLY CRITICAL MELT PERCENTAGE

Weakening of crustal layers may control the style of deformation, as well as the site and the amount of exhumation within orogens (e.g. Beaumont *et al.*, 2001). Anatexis deep in the crust is certainly the primary process enabling a drastic weakening at depth on the scale of an orogen. However, the geological constraints on the amount and consequences of such weakening are based on controversial laboratory experiments performed on centimetre-scale samples. In this paper, we discuss and reinterpret the significance and geological implications of such experiments.

The strength and viscosity of partially melted granite between liquid and solid state vary by 14 orders of magnitude (compilation in Cruden, 1990). The volume proportion of melt, and not the temperature, controls the dramatic strength variation within this interval (e.g. Rutter & Neumann, 1995). Hence, much experimental effort has been invested in examining the relationship between varying melt fraction (Φ) and strength or viscosity of the melt plus solid aggregate.

The first experiments performed under confined (undrained) conditions were designed to investigate the effect of varying melt fraction on the viscosity of partially melted granite (Arzi, 1978). This work showed that the log of bulk viscosity decreases dramatically with melt fraction at $\Phi > 0.1$ (Arzi, 1978; Fig. 1a). However, this conclusion is based on only three samples (Fig. 1a) whose maximum melt fraction was 0.18. No experiments were carried out at higher Φ, yet the semi-empirical law of Roscoe (1952) relating the viscosity of a suspension to the fluid viscosity and solid fraction was used to predict the viscosity of granite magma at $\Phi > 0.26$ (Arzi, 1978; Fig. 1b). The few experimental data of Arzi, together with the Roscoe relationship for a fluid viscosity of 10^4 Pa s (viscosity of the granitic melt used by Arzi, 1978), can be fitted by a sigmoidal curve (Fig. 1) describing the viscosity of granite over the entire range of melt fractions between liquidus and solidus. The drastic viscosity drop at melt fractions between 0.1 and 0.3 was termed the 'rheological critical melt percentage' (RCMP; Fig. 1a) and was inferred to be the melt content at the 'breakdown of the solid and interlocked crystalline skeleton' (Arzi, 1978). This interpretation was apparently confirmed by more detailed deformational experiments on Delegate Aplite with melt fractions up to 0.24 (van der Molen & Paterson, 1979), although the latter study showed that

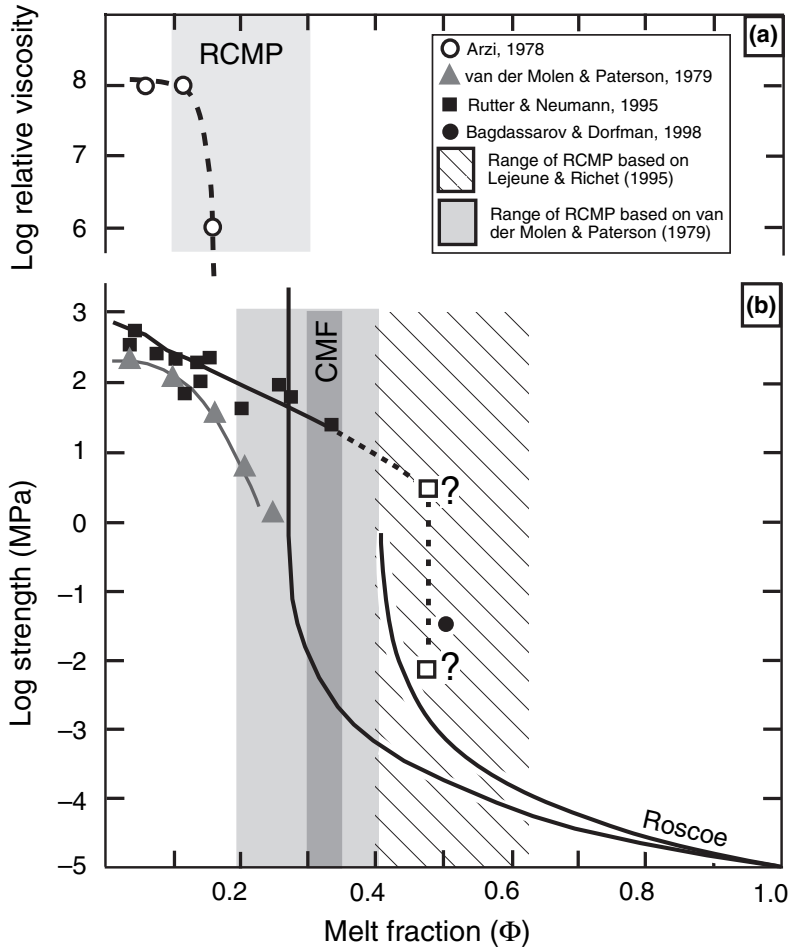

Fig. 1. Logarithmic plots of aggregate strength or effective viscosity *v.* melt fraction. (a) Relative viscosity (sample viscosity/melt viscosity) for Westerly granite (Arzi, 1978). The range of melt fractions corresponding to the RCMP as proposed by Arzi (1978) are shown in light grey. (b) Aggregate strength *v.* melt fraction for Westerly granite (Rutter & Neumann, 1995) and Delegate Aplite (van der Molen & Paterson, 1979). Roscoe's (1952) relationship is plotted (left curve on the diagram) with the shape parameters used in the formulation of Arzi (1978) and with those suggested by Lejeune & Richet (1995). In both cases, a melt viscosity of 10^4 Pa s was used. The Roscoe data are plotted as 'estimated strength' by multiplying strain rate (10^{-5} s^{-1}) by effective viscosity. The range of melt fractions corresponding to the RCMP as constrained by the data of van der Molen & Paterson (1979) and Lejeune & Richet (1995) are shown, respectively, in light grey and with dashed lines. The Critical Melt Fraction (CMF) of van der Molen & Paterson (1979), i.e. the point where the decrease in strength with increasing melt fraction reaches a maximum, is shown in dark grey.

the RCMP occurs at higher Φ (*c.* 0.20–0.40; Fig. 1b). These findings on the RCMP were challenged by Rutter & Neumann (1995) with their deformational experiments on Westerly granite at Φ up to 0.47. Plots of the logarithm of aggregate strength *v.* Φ of these experiments were interpreted to show a linear aggregate strength decrease with increasing Φ (black squares in Fig. 1b).

It is important to note that the experimental devices used for all the experiments cited above could not measure sample strengths of less than 1 MPa. Hence, the sample strengths at $\Phi = 0.2$ in van der Molen & Paterson (1979) and $\Phi = 0.4$ in Rutter & Neumann (1995) are unknown and certainly $\ll 1$ MPa. This limitation may have masked potential deviations from a linear trend of strength *v.* Φ. For example, the strength of the sample containing 0.47 melt fraction in Rutter & Neumann (1995) (open squares in Fig. 1b) could be at any value less than 1 MPa as shown by the question mark in Fig. 1b; a very low value causes the best-fit line to these data to steepen at $\Phi > 0.35$, as predicted by van der Molen & Paterson (1979). Indeed, measurements of the viscosity of a granite magma containing around 50% crystals (Bagdassarov & Dorfman, 1998) indicate that the strength of the samples at these melt fractions is much less than 1 MPa (Fig. 1b).

In order to investigate the viscosity of partially melted silicate materials at $0.3 < \Phi < 1.0$, Lejeune & Richet (1995) carried out a series of uniaxial compression experiments on Mg–Al silicates. These experiments showed a considerable, non-linear drop in viscosity at melt fractions greater than 0.4. This decrease in viscosity is in good agreement with the Roscoe relationship and is associated with a microstructural change in the partially melted material from a framework of interacting and fracturing particles to a suspension of grains in a melt (Lejeune & Richet, 1995). These structural changes are consistent with previous interpretations of the RCMP as the transition from a solid-supported to a liquid-supported aggregate (Arzi, 1978; van der Molen & Paterson, 1979), but this transition was inferred to occur at higher melt fractions (Φ *c.* 0.4–0.6, Fig. 1b) than in the previous investigations.

No additional experiments have been carried out since 1995. Instead, publications have dealt with reinterpretations of the physical processes leading to changes in the viscosity as a function of melt fraction. Vigneresse *et al.* (1996) pointed out that in crystallizing

rocks melt is situated interstitially, i.e. within pockets, whereas during melting it forms intergranular melt films. Hence, for a given Φ, there is less melt interconnection during crystallization than during melting. Therefore, these authors suggested that the RCMP during partial melting and magma crystallization are distinct physical and microstructural phenomena that do not occur over the same range of melt fractions. Renner *et al*. (2000) suggested that aggregate strength measured during the high-strain rate, undrained laboratory experiments on partially melted granite may increase because of dilational hardening, i.e. because of the decrease of pore (melt) pressure as melt leaves the sample during dilation at the onset of fracturing. Takeda & Obata (2003) replotted the experimental data of van der Molen & Paterson (1979) on a linear diagram and inferred a linear relationship between strength and Φ, from which they argued that a RCMP does not exist. In the following, we reinterpret existing experimental data based on a new analysis of strength *v*. Φ diagrams and on consideration of how melt connectivity affects the strength of partially melted rocks.

THE EXPERIMENTAL DATA RECONSIDERED

Following Takeda & Obata (2003), we plot the experimental data of van der Molen & Paterson (1979) on a linear aggregate strength *v*. melt-fraction diagram (Fig. 2a). However, in contrast to Takeda & Obata (2003) and van der Molen & Paterson (1979), we do not plot the average values of several experimental runs, but use all the individual experimental data. These clearly show a non-linear strength decrease as the fraction of melt increases. A dramatic decrease in viscosity takes place between the solidus and Φ of 0.06, such that *c*. 90% of the sample strength is lost over this small range of low melt fractions (steep dashed line in Fig. 2a). For melt fractions $\Phi > 0.06$, the sample strength further decreases with increasing melt content, but with a reduced dependence on melt fraction (shallower dashed line in Fig. 2a). Hence, only 10% of the initial sample strength is lost over this large range of melt fractions ($0.06 < \Phi < 1$, Fig. 2a). The experimental database is not yet sufficient to determine whether the change in the Φ-dependence of aggregate strength is a continuous, exponential function or the intersection of two linear functions with different slopes (Fig. 2a); but the dependence of aggregate strength on the melt fraction clearly changes at Φ around 0.06, in contrast to previous interpretations (Takeda & Obata, 2003).

In order to test whether these aggregate strength *v*. melt-fraction relationships are representative for partially melted continental crust, we also plotted the other experimental data for the strength of partially melted crustal rocks in Fig. 2b (Westerly granite: Rutter & Neumann, 1995; Ivrea Zone amphibolite: Rushmer, 1995; Biotite–plagioclase–quartz orthogneiss: Holyoke & Rushmer, 2002). Deformation of the amphibolite and orthogneiss were carried out in a deformational apparatus with a solid confining medium ('Griggs rig'), whereas the granite and aplite were deformed with a gas-confining medium ('Paterson rig'). Despite these differences, all data sets show trends similar to that of van der Molen & Paterson (1979); (Fig. 2a,b), with curves whose points of maximum curvature are at a Φ of 0.06–0.07. However, the absolute strength values of the different data sets scatter widely, probably because of the different techniques used to generate melting in the samples. van der Molen & Paterson (1979) obtained different amounts of melt in their aplite samples by adding different amounts of water to their starting material. In contrast, Rutter & Neumann (1995) generated different melt contents in their granite samples by varying the temperature. Adding water to the samples reduces the viscosity of the melt, hence also reducing the strength of the samples. This may explain the lower strength of the van der Molen and Paterson samples (Fig. 2a; see also Rutter, 1997 for discussion). The strength of the amphibolite and orthogneiss samples at melt fractions >0.1 are anomalously high, and probably represent the strength of the Alsimag (commercial ceramic) sample jackets rather than of the partially melted aggregates themselves. Alsimag jackets are much stronger than the copper jackets used in the granite and aplite experiments.

The non-linear functions which fit the experimental data in Fig. 2b do not show maximum curvature or change in the range of Φ expected for the RCMP, irrespective of the Φ ranges considered (i.e. Arzi, 1978: 0.1–0.3; van der Molen & Paterson, 1979: 0.2–0.4; Lejeune & Richet, 1995: 0.4–0.6). Even the curve from the Roscoe relationship, which dramatically steepens at $\Phi < 0.50$ on a log diagram (Fig. 1b), does not depart discernibly from the horizontal axis in Fig. 2b. The strength drop at the RCMP may be greater than five orders of magnitude (e.g. fig. 15 of Lejeune & Richet, 1995), but its absolute value must be <1 MPa, which is the maximum possible strength of partially melted granites before the melt fraction exceeds 0.25 (i.e. the RCMP is attained) in deformational experiments (Fig. 2b; van der Molen & Paterson, 1979; Rutter & Neumann, 1995). Thus, the strength drop at the RCMP is *c*. three orders of magnitude less than the strength drop that occurs between the solidus and a melt fraction Φ of 0.07. For this reason, the strength drop at the RCMP is too small to be seen on a linear plot of strength *v*. fraction of melt for partially melted granite. Logarithmic plots expand and visibly accentuate the low strength part of the diagram, but compress the upper part. This is why the RCMP always appears as a first-order rheological transition in the traditional logarithmic aggregate strength *v*. melt-fraction plots (Arzi, 1978; van der Molen & Paterson, 1979; Wickham, 1987; Cruden, 1990), but is invisible on a linear plot unless the scale of the strength axis is adjusted appropriately (inset of Figs 3 & 4).

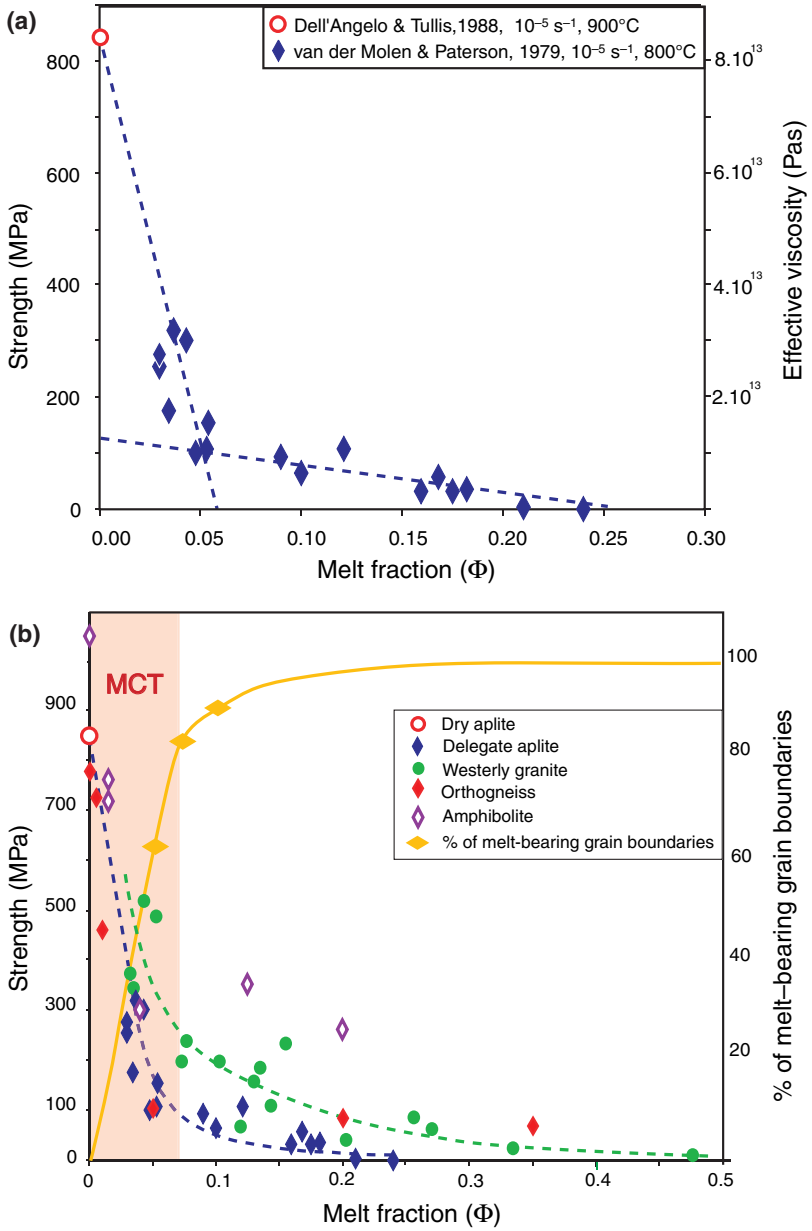

Fig. 2. Linear plots of aggregate strength *v.* melt fraction. (a) Linear fit of experimental data: Partially melted Delegate Aplite from van der Molen & Paterson (1979). The strength of solid, melt-free granite is taken from Dell'Angelo & Tullis (1988). The data are fitted by two linear functions intersecting at Φ of *c.* 0.06. However, continuous exponential functions may also satisfactorily fit the data (see b). (b) Compilation of strength data for Delegate Aplite (van der Molen & Paterson, 1979), Westerly granite (Rutter & Neumann, 1995), Ivrea amphibolite (Rushmer, 1995) and orthogneiss (Holyoke & Rushmer, 2002). Trend lines are least squares exponential fits of Delegate Aplite and Westerly granite. The strength data for the amphibolites, orthognesiss, and dry aplite samples were obtained from deformational rigs with solid confining media, in contrast to the gas-confining medium used to measure the strength of partially melted Delegate Aplite and Westerly granite. Solid line: percentage of melt-bearing grain boundaries as obtained from data of a static melting experiment of van der Molen & Paterson (1979).

In contrast, the much greater strength-drop between the solidus and a melt fraction Φ of 0.07, is invisible on the logarithmic aggregate strength *v.* melt-fraction plots (Fig. 1). We interpret this greater strength drop to be a melt-connectivity transition (MCT), as discussed below. From a microstructural point of view, the upper boundary of the MCT corresponds to the permeability threshold of Maaløe & Scheie (1982) and to the 'liquid percolation threshold' (LPT) of Vigneresse *et al.* (1996). However, it is emphasized that the MCT is a rheological transition defined on the basis of experimental data, and not a segregation threshold as that of Maaløe & Scheie (1982), or the LPT of Vigneresse *et al.* (1996). The melt content at the transition from a solid-supported to a liquid-supported structure has a subordinate effect on strength and is therefore not really the rheologically critical one. Therefore, the term RCMP is misleading and we suggest that it be replaced by the term 'solid-to-liquid transition' (SLT). The transition which is truly critical to rheology is the MCT (Fig. 4).

DISCUSSION

Causes of the drastic strength drop at $0.0 < \Phi < 0.07$

Point counting of melt pockets in thin sections from static experiments shows that the proportion of grain boundaries containing melt increases non-linearly between $\Phi = 0.0$ and $\Phi = 1$ (van der Molen & Paterson,

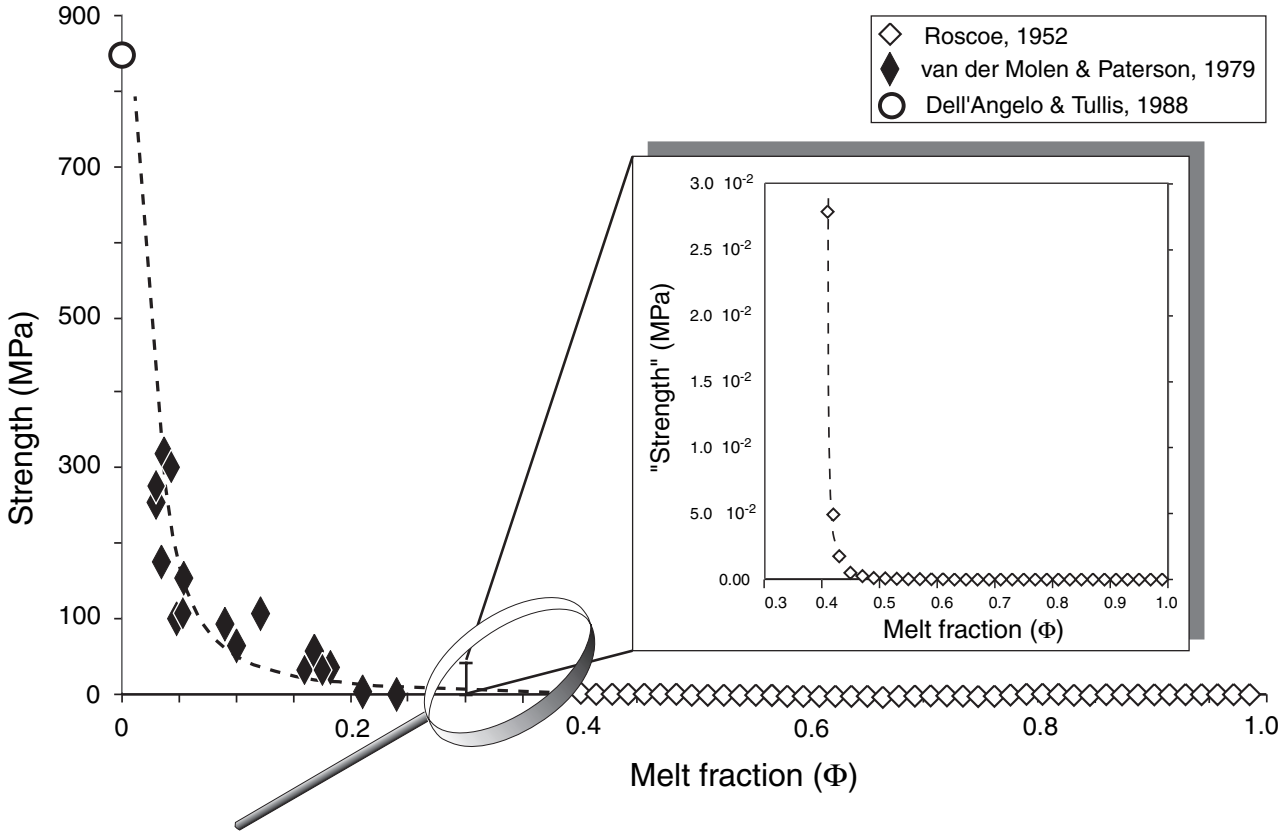

Fig. 3. Linear plot of aggregate strength *v.* melt fraction of partially melted Delegate Aplite (van der Molen & Paterson, 1979) containing the Roscoe (1952) relationship calculated for a melt viscosity of 10^4 Pa s. Strength is estimated as in Fig. 1. The RCMP is not visible in this diagram because of the enormous difference between experimentally measured strength at melt fractions < 0.25 and the strength estimated from the Roscoe (1952) relationship at melt fractions > 0.4.

1979; Fig. 2b). This proportion increases dramatically at melt fractions between 0.0 and 0.1, such that at $\Phi = 0.1$, 90% of boundaries contain melt (van der Molen & Paterson, 1979). As the melt fraction further increases Φ-value from 0.1 to 1, the number of boundaries with melt hardly increases at all (Fig. 2b) while the melt films at the boundaries necessarily become thicker. Interestingly, the sharpest bend in the curve for the proportion of melt-bearing boundaries coincides with the sharpest bend of the aggregate strength curve (Fig. 2b); at melt fractions greater than 0.07, both curves flatten out. This coincidence in the shapes and slopes of the two curves suggests that the increasing proportion of melt-bearing grain boundaries is the cause of the reduction of aggregate strength at the MCT.

Two lines of reasoning suggest that both the solid grains and the melt phase are continuously interconnected to melt fractions of up to 0.07, at the upper boundary of the MCT. First, deformational experiments show that melt fractions of 0.06–0.07 are too small to induce the breakdown of the solid framework, but sufficient to establish three-dimensional melt interconnectivity (Bruhn *et al.*, 2000). This is consistent with the behaviour of granular materials with a random-packing density, in which the breakdown of the solid framework only occurs in the range $\Phi = 0.35$–0.40 (van der Molen & Paterson, 1979). Second, the stress–strain curves in the experiments show that even after strength drops upon attainment of the MCT, residual sample strengths remain relatively high (> 50 MPa for Delegate Aplite, > 200 MPa for Westerly granite; Fig. 2b). Such residual strength values are far above those of a granitic melt and indicate that bulk stress is still supported by the solid framework. Therefore, we believe that both the melt phase and the solid grains are interconnected when a melt fraction of around 0.07 is reached. Increasing the melt fraction above 0.07 causes melt channels to widen, hence further weakening the rock, but without fundamentally changing its structure. A change in structure corresponding to the breakdown of the solid framework occurs when the SLT is reached at $\Phi = 0.35$.

Under static conditions, melt fractions as small as 0.004 are sufficient to form an interconnected network of granitic melt in texturally equilibrated quartzitic aggregates (Laporte *et al.*, 1997). However, we believe that the partially melted aplitic samples of van der Molen & Paterson (1979) never attained complete textural equilibrium, because they were heated for only 2 h above the solidus, under static conditions.

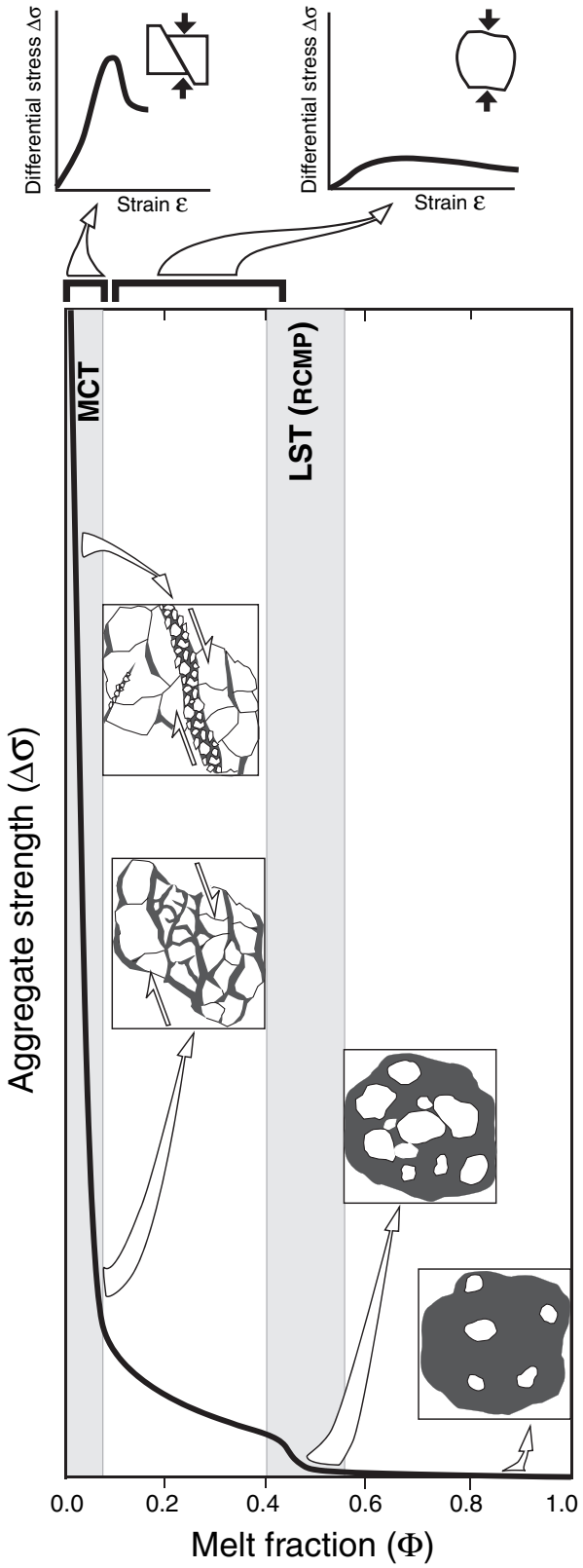

Dell'Angelo & Tullis (1988) observed that textural equilibrium in natural aplites with even smaller grain size was not attained, even after several days. Under static conditions, non-texturally equilibrated rocks may require melt fractions between 0.08 and 0.11 to attain melt-interconnection (Cheadle *et al.*, 2004). This value is higher than $\Phi = 0.07$ marking the upper boundary of the MCT (Fig. 2b). However, melt fractions of only 0.07 enable the formation of interconnected networks of melt under dynamic conditions, as shown by recent deformational experiments (Bruhn *et al.*, 2000). Therefore, the change in the Φ-dependence of aggregate strength corresponding to the maximum curvature of the strength curves in Fig. 2 seems to coincide with the attainment of melt interconnection.

The maximum curvature of the strength curves at $\Phi = 0.07$ also coincides systematically with a change in the shape of the stress–strain curves, as synopsized from the experiments in the insets to Fig. 4. The sharp drop in aggregate strength for samples deformed at $\Phi < 0.07$ is diagnostic of brittle failure, sometimes followed by limited cataclastic flow at residual strength, whereas the broader, flatter curves for samples at $\Phi > 0.07$ are typical of ductile yielding and flow (e.g. see fig. 4 of van der Molen & Paterson, 1979). Hence, a major transition in the dominant deformation mechanism is inferred to occur at $\Phi = 0.07$.

Inferring the mechanisms of weakening in the experiments is difficult because the microstructures pictured in the literature invariably formed at various stages of the stress–strain history of a given sample, sometimes after the attainment of peak stress. The sample strength *v.* melt-fraction curves showing the melt-dependent weakening are constructed from measurements of peak stress. Yet, based on the authors' comparisons of microstructures in the low-strain samples deformed below the MCT with those in the high-strain samples deformed above the MCT (van der Molen & Paterson, 1979; Rutter & Neumann, 1995) we are able to infer some of the possible mechanisms of weakening.

Fig. 4. Schematic plot of aggregate strength *v.* melt fraction for partially melted granite between the liquidus and solidus. Note the two steep segments of the strength curve corresponding to the MCT and to the LST (or RCMP). The vertical scale of the lower part of the ordinate is exaggerated in order to make the LST visible. Generic stress–strain curves for the MCT and LST are shown at the top of the figure, based on the mechanical data of van der Molen & Paterson (1979). The microstructural sketches illustrate deformation at different melt fractions. At Φ around 0.03, deformation localizes along a melt-bearing fault. At $\Phi = 0.07$, deformation is more distributed on the sample scale, but it is localized along the interconnected network of melt on the grain scale. At $0.4 = \Phi = 0.6$ the solid framework breaks down, but grain interactions still occur. At $\Phi = 0.6$ the solid particles are suspended in the melt and do not interact with each other.

Weakening at $0 < \phi < 0.07$ probably involves localized, inter- and intragranular microcracking, as well as limited rigid-body rotation of grains and grain aggregates accommodated by frictional sliding and movement along incipient melt pockets (see figs 8–10 in van der Molen & Paterson, 1979; fig. 9 in Rutter & Neumann, 1995). Intergranular microcracking is favoured during melting by an increase in pore melt pressure and a corresponding decrease in effective normal stress in the aggregates. Dislocation motion and diffusional processes at grain boundaries are probably subordinate, if at all present, as they are too slow to accommodate the observed deformation at the high laboratory strain rates. This is confirmed by the absence of microstructural evidence for either dislocation mobility or diffusion-accommodated grain-boundary sliding, even in the 'wet' experiments of van der Molen & Paterson (1979).

The less-pronounced, melt-dependent weakening at $\phi > 0.07$ and up to about the SLT at $\phi = 0.4$ is attributed to viscous melt flow within interconnected melt domains. Once the melt films have become interconnected, deformation is partitioned into these weak layers, which widen with increasing melt content. Microstructural observations of samples with melt fractions greater than 0.07 also point to fracturing, but involving a more distributed type of deformation and less pronounced grain-size reduction (van der Molen & Paterson, 1979; Rutter & Neumann, 1995). Therefore, the steeper part of the strength *v.* melt-fraction curve reflects primarily a fundamental structural change as a melt network is established, whereas the flatter part of this curve reflects only the volumetric increase of the networked weak phase (melt).

Rheology of crystallizing *v.* melting rocks

Several studies have argued that the rheology of melting rocks differs from that of crystallizing rocks and that the concept of an RCMP may only apply to crystallizing rocks (Vigneresse *et al.*, 1996; Vigneresse & Tikoff, 1999; Burg & Vigneresse, 2002; Takeda & Obata, 2003). This conclusion is based on the idea that the distribution of melt in crystallizing and melting rocks is different (Vigneresse *et al.*, 1996). According to this idea, melting under static conditions induces intergranular films, whereas melt crystallizing under static conditions is distributed within pockets whose shape and location is determined by the shape and position of the crystallizing minerals. For a given melt fraction less than 0.4, melt interconnectivity is much higher in a melting system than in a crystallizing one (Vigneresse *et al.*, 1996). However, numerous experiments have shown that melt distribution in deforming silicate aggregates with melt fractions less than 0.4 is controlled by the orientation and magnitude of the applied stress (e.g. Daines & Kohlstedt, 1997; Gleason *et al.*, 1999) and/or by the crystallographic-preferred orientation and shape-preferred orientation of the solid grains (Kohlstedt & Zimmerman, 1996). Therefore, for rocks undergoing deformation at melt fractions less than 0.4, the melt topology will be determined by differential stress and finite strain (Daines & Kohlstedt, 1997), irrespective of the melting or crystallizing state of the rock. This interpretation is supported by experimental evidence from partially melted ultramafic (review in Daines & Kohlstedt, 1997) and granitic (e.g. review in Rosenberg, 2001) rocks.

At laboratory conditions, the application of a differential stress induces melt redistribution within hours (e.g. Gleason *et al.*, 1999). Therefore, Handy *et al.* (2001) and Rosenberg (2001) predicted that melt distribution in melting and in crystallizing systems can only be different if melting and/or crystallization are very rapid, i.e. faster than the rate of stress-induced microstructural equilibration. This may occur in subvolcanic or plutonic rocks cooling in shallow crustal levels, but not deep in the crust. This is born out by several investigations showing that melt in deep-seated, naturally deforming and crystallizing rocks with low melt fractions (< 0.2) is distributed as intergranular films (Rosenberg & Riller, 2000; Sawyer, 2001a). The same type of melt topology is described for rocks undergoing melting (e.g. Sawyer, 2001b). Therefore, the MCT, which is observed at melt fractions as small as 0.07, is expected to exist both during initial melting and during the final stages of crystallization.

In this context, we point out that the experimental database used to define the MCT or, for that matter, any of the other rheological thresholds previously proposed (e.g. the RCMP) was obtained from samples deformed in the presence of different, but constant melt fractions. The samples were heated above their solidus at static conditions for *c.* 2 h before being deformed (van der Molen & Paterson, 1979). Therefore, the melt fraction did not increase (or decrease) during any of the deformational runs. In addition melt distribution in the deformed samples indicates that melt moved from cracks and grain boundaries oriented at high angle to the maximum compressive principal stress, to grain boundaries and cracks subparallel to the principal compressive stress (van der Molen & Paterson, 1979). Hence, melt topology in these experiments was controlled by the orientation and shape of the stress ellipsoid. The point made here is that there is no reason to restrict inferences about rheological transitions in these experiments to rocks undergoing melting; the experiments allow speculation about thresholds in crystallizing systems as well.

GEOLOGICAL IMPLICATIONS AND EXPERIMENTAL LIMITATIONS

The discussion above shows that some aspects of the experimental rheology of partially melted rocks have

been erroneously interpreted. A very important dynamic, rheological transition at very low melt fractions (the MCT at Φ around 0.07) has been overlooked, whereas the significance of a lesser strength drop at higher melt fraction (the SLT at $0.2 < \Phi < 0.5$) has been overemphasised. Our interpretation implies that the onset of syntectonic melting coincides with a drastic weakening of the continental crust, whereas a further increase in melt content results in more modest weakening.

The extrapolation of these results to natural conditions in the lithosphere remains difficult for the following reasons. (1) There is still no reliable flow law with which to extrapolate existing experimental data to much slower, natural strain rates (10^{-11}–10^{-14} s^{-1}). In fact, none of the existing rheological data on partially melted crustal rocks was obtained from steady state experiments. The strength of melt-free, quartzo-feldspathic rock undergoing power-law creep at natural strain rates and near-solidus temperatures is on the order of one to tens of MPa only (Carter & Tsenn, 1987; Kohlstedt *et al*., 1995), so that the relative strength of melt-free and melt-bearing rocks is not large, if at all significant. Thus, the strength drop observed at $\Phi < 0.07$ in experiments may be much more modest in nature than measured in the laboratory. (2) The dominant deformation mechanism in all of the experiments was cataclastic flow, yet in nature, crustal rocks deform by viscous creep in the presence of melt (Rosenberg, 2001) However, it is interesting to note that mantle rocks experimentally deformed by viscous creep in the presence of melt fractions between 0.0 and 0.12 show the same trend described in Fig. 2 for crustal rocks (Hirth & Kohlstedt, 2003), with a major discontinuity at a melt fraction of *c*. 0.06. (3) The rheological data for partially melted rocks were obtained at coaxial shortening strains of only 1–6%. The strength of partially melted rocks at higher strains has not been investigated yet. We note, however, that the data of Rutter & Neumann (1995) allow the strength of the samples to be plotted against the melt fraction for a strain value of 8%, i.e. well beyond the point of maximum strength. Even at these relatively high strain values, the strength *v*. melt-fraction curves show a trend similar to that plotted in Fig. 3. Hence, the effect of strain may not fundamentally modify the critical melt fraction at which the MCT occurs. (4) The generation of small amounts of liquid in the sealed experiments results in a melt pressure that is most likely about equal to the imposed confining pressure. Therefore, all experiments so far may be considered in some ways to have been effectively unconfined (Renner *et al*., 2000). Drained experiments are needed in order to obtain an effective confinement. (5) Dilatancy hardening may have increased the strength of melt-bearing samples in some deformational experiments (Renner *et al*., 2000), but this process is not expected to occur at slower strain rates in nature (Brace & Martin, 1968) where more time is available to re-equilibrate pore pressure following short-term perturbations induced by dilation.

CONCLUSIONS

Extrapolation of the existing deformational experiments on partially melted crustal rocks to natural conditions remains speculative because of the lack of experiments performed at controlled melt pressure under conditions favouring steady state in the dislocation or diffusion creep regime. Existing experiments allow us to infer that the strength of partially melted rocks between the liquidus and solidus is characterized by two pronounced discontinuities. (1) A sharp discontinuity at the upper boundary of the 'melt connectivity transition' or MCT (Fig. 4) at a melt fraction around 0.07. The MST corresponds to a change in the rock microstructure from a dry (melt-free) aggregate to an aggregate containing a network of highly interconnected melt channels. (2) The more modest discontinuity at the 'solid-to-liquid transition' or SLT at a melt fraction around 0.4. The SLT corresponds to the break down of the solid framework (the RCMP of Arzi, 1978), i.e. to a microstructural transition from a solid framework containing a through-going network of melt channels to a suspension of isolated grains in a melt (i.e. a magma). At the MCT, the rock strength changes by less than two orders of magnitude (Fig. 2b), whereas at the SLT this change may be larger than five orders of magnitude (Lejeune & Richet, 1995). However, the absolute strength drop at the SLT ($\ll$1 MPa) is negligible compared with that at the MCT (around 750 MPa; Figs 2 & 3). Since its inception, the RCMP has been interpreted as a range of melt fractions over which 'most of the extreme change of large-strain viscosities' occurs (Arzi, 1978). Our analysis of the experimental data shows that this extreme change occurs at the MCT at much lower melt fractions than at the RCMP (Figs 3 & 4). The name RCMP is therefore a misnomer and we suggest replacing it with the more neutral term SLT.

In view of the good correlation between the proportion of melt-bearing grain boundaries and the magnitude of strength reduction, we argue that the increasing degree of melt-film interconnection, rather than the break-up of the solid framework, controls the greatest strength drop in partially melted rocks. The dramatic strength drop at $0 < \Phi < 0.07$, irrespective of the melting or crystallizing state of the rock, suggests that localization of deformation takes place as soon as melting starts. Conversely, drastic hardening is expected during the very last stages of crystallization. The mechanical response of crust containing an anatectic layer with 8% melt may be very different from one that contains only 2% melt, but will not differ fundamentally from that of crust containing a layer with 50% melt, despite their different microstructures and compositions (e.g. Sawyer, 1998). The SLT does

not need to be attained for there to be pronounced weakening and partitioning of deformation in a melting region. Changes in the melt fraction across the SLT may be important for the dynamics of magma chambers, where flow is expected to localize in parts of the chamber where the crystal fraction locally increases above, or decreases below 0.5. However, the absolute change of strength across the SLT is too small (< 1 MPa) to affect the mechanical behaviour of continental crust.

ACKNOWLEDGEMENTS

Financial support from the Deutsche Forschungsgemeinschaft (Ro 2177/1-1) is acknowledged. We thank M. Brown, for editorial assistance. We appreciate the constructive reviews of T. Rushmer, and E. Sawyer, as well as the negative assessment of J. Renner. The latter nevertheless strengthened our conviction that existing experiments contain much more information than meets the eye at first glance!

REFERENCES

Arzi, A., 1978. Critical phenomena in the rheology of partially melted rocks. *Tectonophysics*, **44,** 173–184.

Bagdassarov, N. & Dorfman, A.M., 1998. Viscoelastic behaviour of partially molten granites. *Tectonophysics*, **290,** 27–45.

Beaumont, C., Jamieson, R.A., Nguyen, M.H. & Lee, B., 2001. Himalayan tectonics explained by extrusion of a low-viscosity crustal channel coupled to focused surface denudation. *Nature*, **414,** 738–742.

Brace, W.F. & Martin, R.J., 1968. A test of the law of effective stress for crystalline rocks of low porosity. *International Journal of Rock Mechanics and Mineral Sciences*, **5,** 415–426.

Bruhn, D., Groebner, N. & Kohlstedt, D., 2000. An interconnected network of core-forming melts produced by shear deformation. *Nature*, **403,** 883–886.

Burg, J.-P. & Vigneresse, J.-L., 2002. Non-linear feedback loops in the rheology of cooling-crystallizing felsic magma and heating-melting felsic rock. In: *Deformation Mechanisms, Rheology and Tectonics: Current Status and Future Perspectives*. (eds. De Meer, S., Drury, M.R., De Bresser J.H.P. & Pennock, G.M.). *Geological Society of London, Special Publication*, **200,** 275–292.

Carter, N.L. & Tsenn, M.C., 1987. Flow properties of continental lithosphere. *Tectonophysics*, **136,** 27–63.

Cheadle, M.J., Elliott, M.T. & McKenzie, D., 2004. Percolation threshold and permeability of crystallizing igneous rocks: the importance of textural equilibrium. *Geology*, **32,** 757–760.

Cruden, A.R., 1990. Flow and fabric development during the diapiric rise of magma. *Journal of Geology*, **98,** 681–698.

Daines, M.J. & Kohlstedt, D.L., 1997. Influence of deformation on melt topology in peridotites. *Journal of Geophysical Research*, **102,** 10257–10271.

Dell'Angelo, L. & Tullis J., 1988. Experimental deformation of partially melted granitic aggregates. *Journal of metamorphic Geology*, **6,** 495–515.

Gleason, G.C., Bruce, V. & Green, H.W., 1999. Experimental investigation of melt topology in partially molten quartzofeldspathic aggregates under hydrostatic and non hydrostatic stress. *Journal of metamorphic Geology*, **17,** 705–722.

Handy, M.R., Mulch, A., Rosenau, M. & Rosenberg, C.L., 2001. A synthesis of the role of fault zones and melts as agents of weakening, hardening and differentiation of the continental crust. In: *The Nature and Tectonic Significance of Fault Zone Weakening*. (eds. Holdsworth, R.E., Strachan, R.A., Magloughlin J.F. & Knipe R.J.), *Geological Society of London, special publication*, **186,** 305–332.

Hirth, G. & Kohlstedt, D., 2003. Rheology of the upper mantle and the mantle wedge: A view from the Experimentalists. *Geophysical Monograph*, **138,** 83–105.

Holyoke, C.W. & Rushmer, T., 2002. An experimental study of grain scale melt segregation mechanisms in two common crustal rock types. *Journal of metamorphic Geology*, **20,** 493–512.

Kohlstedt, D.L. & Zimmerman, M., 1996. Rheology of partially molten mantle rocks. *Annual Review of Earth and Planetary Sciences*, **24,** 41–62.

Kohlstedt, D.L., Evans, B. & Mackwell, S.J., 1995. Strength of the lithosphere: Constraints imposed by laboratory experiments. *Journal of Geophysical Research*, **100,** 17587–17602.

Laporte, D., Rapaille, C. & Provost, A., 1997. Wetting angles, equilibrium melt geometry, and the permeability threshold of partially molten crustal protholiths. In: *Granite: From Segregation of Melt to Emplacement Fabrics*. (eds. Bouchez, J.L., Hutton, D.H.W. & Stephens, W.E.), pp. 31–54. Kluwer Academic publishers, Dordrecht.

Lejeune, A. & Richet P., 1995. Rheology of crystal-bearing silicate melts: an experimental study at high viscosities. *Journal of Geophysical Research*, **100,** 4215–4229.

Maaløe, S. & Scheie, Å, 1982. The permeability-controlled accumulation of primary magma in a planetary mantle. *Physics of The Earth and Planetary Interiors*, **29,** 344–353.

van der Molen, I. & Paterson, M.S., 1979. Experimental deformation of partially-melted granite. *Contributions to Mineralogy and Petrology*, **70,** 299–318.

Renner, J., Evans, B. & Hirth, G., 2000. On the rheologically critical melt fraction. *Earth and Planetary Science Letters*, **181,** 585–594.

Roscoe, R., 1952. The viscosity of suspensions of rigid spheres. *British Journal of Applied Physics*, **3,** 267–269.

Rosenberg, C.L., 2001. Deformation of partially-molten granite: a review and comparison of experimental and natural case studies. *International Journal of Earth Sciences*, **90,** 60–76.

Rosenberg, C.L. & Riller, U., 2000. Partial melt topology in statically and dynamically recrystallized granite. *Geology*, **28,** 7–10.

Rushmer, T., 1995. An experimental deformation study of partially molten amphibolite: application to low-melt fraction segregation. *Journal of Geophysical Research*, **100,** 15681–15695.

Rutter, E., 1997. The influence of deformation on the extraction of crustal melts: a consideration of the role of melt-assisted granular flow. In: *Deformation-enhanced fluid transport in the Earth's crust and mantle*. (ed. Holness, M.), *The Mineralogical Society Series*, **8,** 82–110.

Rutter, E. & Neumann, D.H.K., 1995. Experimental deformation of partially molten Westerly granite under fluid-absent conditions, with implications for the extraction of granitic magmas. *Journal of Geophysical Research*, **100,** 15697–15715.

Sawyer, E.W., 1998. Formation and evolution of granite magmas during crustal reworking: the significance of diatexites. *Journal of Petrology*, **39,** 1147–1167.

Sawyer, E.W., 2001a. Grain-scale and outcrop-scale distribution and movement of melt in a crystallizing granite. *Transactions of the Royal Society of Edinburgh Earth Sciences*, **91,** 73–85.

Sawyer, E.W., 2001b. Melt segregation in the continental crust: distribution and movement of melt in anatectic rocks. *Journal of metamorphic Geology*, **19,** 291–309.

Takeda, Y.-T. & Obata, M., 2003. Some comments on the rheologically critical melt percentage. *Journal of Structural Geology*, **25,** 813–818.

Vigneresse, J.-L. & Tikoff, B., 1999. Strain partitioning during partial melting and crystallizing felsic magmas. *Tectonophysics*, **312,** 117–132.

Vigneresse, J.-L., Barbey, P. & Cuney, M., 1996. Rheological transitions during partial melting and crystallization with application to felsic magma segregation and transfer. *Journal of Petrology*, **37,** 1579–1600.

Wickham, S.M., 1987. The segregation and emplacement of granitic magmas. *Journal of the Geological Society, London*, **144,** 281–297.

Received 1 September 2004; Revision Accepted 10 November 2004.